



Network analysis reveals a causal role of mitochondrial gene activity in atherosclerotic lesion formation



Baiba Vilne^{a, b}, Josefin Skogsberg^c, Hassan Foroughi Asl^c, Husain Ahammad Talukdar^{c, d}, Thorsten Kessler^{a, b}, Johan L.M. Björkegren^{c, e, f, g, **}, Heribert Schunkert^{a, b, *}

^a Deutsches Herzzentrum München, Klinik für Herz- und Kreislauferkrankungen, Technische Universität München, Munich, Germany

^b DZHK (German Research Centre for Cardiovascular Research), Munich Heart Alliance, Munich, Germany

^c Cardiovascular Genomics Group, Division of Vascular Biology, Department of Medical Biochemistry and Biophysics, Karolinska Institutet, Stockholm, Sweden

^d Integrated Cardio Metabolic Center (ICMC), Karolinska Institutet, 141 57 Huddinge, Sweden

^e Department of Physiology, Institute of Biomedicine and Translation Medicine, University of Tartu, Estonia

^f Department of Genetics and Genomic Sciences, Icahn Institute for Genomics and Multiscale Biology, Icahn School of Medicine at Mount Sinai New York, New York, USA

^g Clinical Gene Networks AB, Stockholm, Sweden

ARTICLE INFO

Article history:

Received 24 May 2017

Received in revised form

5 October 2017

Accepted 18 October 2017

Available online 21 October 2017

Keywords:

Atherosclerosis

Co-expression network

Gene expression

Hypercholesterolemia

Mitochondria

Systems biology

ABSTRACT

Background and aims: Mitochondrial damage and augmented production of reactive oxygen species (ROS) may represent an intermediate step by which hypercholesterolemia exacerbates atherosclerotic lesion formation.

Methods: To test this hypothesis, in mice with severe but genetically reversible hypercholesterolemia (i.e. the so called Reversa mouse model), we performed time-resolved analyses of mitochondrial transcriptome in the aortic arch employing a systems-level network approach.

Results: During hypercholesterolemia, we observed a massive down-regulation (>28%) of mitochondrial genes, specifically at the time of rapid atherosclerotic lesion expansion and foam cell formation, i.e. between 30 and 40 weeks of age. Both phenomena - down-regulation of mitochondrial genes and lesion expansion - were largely reversible by genetically lowering plasma cholesterol (by >80%, from 427 to 54 ± 31 mg/L) at 30 weeks. Co-expression network analysis revealed that both mitochondrial signature genes were highly connected in two modules, negatively correlating with lesion size and supported as causal for coronary artery disease (CAD) in humans, as expression-associated single nucleotide polymorphisms (eSNPs) representing their genes overlapped markedly with established disease risk loci. Within these modules, we identified the transcription factor estrogen related receptor (ERR)- α and its co-factors PGC1- α and - β , i.e. two members of the peroxisome proliferator-activated receptor γ co-activator 1 family of transcription regulators, as key regulatory genes. Together, these factors are known as major orchestrators of mitochondrial biogenesis and antioxidant responses.

Conclusions: Using a network approach, we demonstrate how hypercholesterolemia could hamper mitochondrial activity during atherosclerosis progression and pinpoint potential therapeutic targets to counteract these processes.

© 2017 The Authors. Published by Elsevier Ireland Ltd. This is an open access article under the CC BY-NC-ND license (<http://creativecommons.org/licenses/by-nc-nd/4.0/>).

1. Introduction

Coronary artery disease (CAD) remains the leading cause of death (see WHO <http://www.who.int/en/>). Hypercholesterolemia, its major risk factor, has been associated with exacerbated production of reactive oxygen species (ROS) [1,2], which significantly contributes to the initiation and development of atherosclerotic lesions [3]. Mitochondria are the main intracellular source of ROS

* Corresponding author. Deutsches Herzzentrum München, Technische Universität München, Lazarettstr. 36, 80636 Munich, Germany.

** Corresponding author. Department of Genetics and Genomic Sciences, Icahn Institute for Genomics and Multiscale Biology, Icahn School of Medicine at Mount Sinai, One Gustave L. Levy Place - Box 1498, New York, NY 10029-6574, USA.

E-mail addresses: johan.bjorkegren@mssm.edu (J.L.M. Björkegren), schunkert@dhm.mhn.de (H. Schunkert).

and also the main targets, when ROS are produced exceedingly [4]. Accumulation of damaged mitochondrial components even further increases ROS production [5], triggering inflammatory responses and cell death [6]. Two important mitochondrial systems counteract these processes: (i) powerful antioxidant systems to carefully control the levels of ROS [6] and (ii) essential quality control mechanisms to maintain mitochondrial 'fitness' and replenish damaged components - mitochondrial biogenesis [4]. Moreover, mitochondrial abundance is dynamically regulated in response to a wide range of cues, such as diet and ROS production [7]. This complex fine-tuning involves close communication with the nucleus, requiring coordinated transcription of nuclear and mitochondrial genes [4]. The mitochondrial genome encodes only 37 genes, mainly components of the OXPHOS machinery [5], whereas the remaining ~1000–1500 mitochondrial proteins are all encoded by the nuclear genome [7].

We hypothesize that one way in which hypercholesterolemia increases ROS and accelerates atherogenesis is by hampering mitochondrial function, which would be likely reflected by changes in mitochondrial transcription patterns. To address this question, we used the so called Reversa mouse model with human-like hypercholesterolemia. In these mice, LDL receptor-deficiency and apo-B100 knock-in (*Ldlr*^{-/-} *ApoB*^{100/100}) results in large numbers of small lipoproteins, leading to spontaneous and rapid atherosclerosis development even on a chow diet. Whereas an additional genetic switch allows to inhibit hepatic synthesis of lipoproteins (*Mttp*^{flox/flox} *Mx1-Cre*) and abrupt plasma cholesterol-lowering [8]. Previously, we have thoroughly investigated different stages of atherosclerotic lesion development and their response to plasma cholesterol-lowering in the Reversa mouse model and generated transcriptome data from the whole-tissue homogenates of their aortic arches, at each time point [9,10].

In this study, we applied a three-step systems-level analysis to explore the mitochondrial adaptive responses to hypercholesterolemia in these mice. We first identified critical mitochondrial signatures changing during lesion expansion and after cholesterol lowering, which we then explored in the network context of tightly co-expressed sets of genes (i.e. modules). We further correlated these modules to changes in atherosclerotic lesions size over time and integrated them with established CAD risk loci from human genome-wide association studies (GWAS) [11] via expression-related SNPs, to predict their disease causality. Finally, by focusing on transcription regulators involved in ROS homeostasis pathways, we identified *ERR-α* and its co-factors *PGC1-α* and *-β* - as key regulatory genes driving mitochondrial responses to hypercholesterolemia, leading to rapid atherosclerotic lesion expansion.

2. Materials and methods

2.1. Mitochondrial signature gene identification

We used microarray data generated by Björkegren and colleagues as described in detail in the [Supplemental Methods](#) and in Refs. [9,10]. In brief, mice fed rodent chow containing 4% fat were sacrificed at 10, 20, 30, 40 weeks of age (*n* = 7, 5, 6 and 5, respectively). In an additional test group of 30-week-old mice (*n* = 6), plasma cholesterol was genetically lowered (by >80%, from 427 to 54 ± 31 mg/L). For this, mice were injected with 500 μl of pl-pC (1 μg/μl; Sigma, St. Louis, MO) every other day for 6 days to induce Cre expression and recombination of *Mttp*. In all cases, the aortic arch from above the third rib to the aortic root was removed and homogenized with FastPrep (Qbiogene, Irvine, CA), total RNA was isolated with RNeasy Mini Kit (Qiagen) and quality assessed with a Bioanalyzer 2100 (Agilent Technologies, Santa Clara, CA). Transcriptomes were profiled with Mouse Genome 430 2.0

GeneChips cDNA arrays (Affymetrix, Santa Clara, CA). After microarray data pre-processing and quality control using R/Bioconductor [12] packages *affy* [13], *gcrma* [14] and *arrayQualityMetrics* [15], we obtained a set of 9512 expressed genes ([Supplemental Table 2](#) and [Fig. 5](#)). Pair-wise (e.g., week 30 vs. 40) differential expression analysis was conducted using *limma* [16] and corrected for multiple testing using the Benjamini-Hochberg false discovery rate (FDR) [17]. To define mitochondrial genes, we made use of the Gene Ontology (GO) [18] annotations (*n* = 1658; [Supplemental Table 1](#)). Further filtering resulted in a smaller set of expressed mitochondrial genes (*n* = 1240; [Supplemental Table 2](#)). Fisher's exact test [19] was used to calculate the overlaps between the gene sets.

2.2. WGCNA co-expression network analysis

We constructed gene co-expression networks from the 9512 genes by performing the weighted gene co-expression network analysis (WGCNA) [20]. Pearson's gene-gene correlations were first calculated and converted into connection strength by fitting an index (R^2) to evaluate a scale-free network structure. Thereafter, genes were grouped based on a measure of neighborhood sharing, i.e. the topological overlap of their connectivity using average linkage hierarchical clustering. To detect smaller sub-groups of highly connected genes (modules), the dynamic tree cut algorithm was applied to cut the branches of the dendrogram into modules with a minimum size of 30 genes. These modules were further summarized into the so called module eigengenes (MEs), i.e. the first principal component of a given module, which can be considered as representatives of the transcription profiles in that module. To quantify module-trait associations, the MEs were correlated (Pearson's test) to mouse phenotype traits from Ref. [9] ([Figs. 1 and 2](#) and [Supplemental Fig. 8, Supplemental Table 7](#)), with a particular focus on changes in atherosclerotic lesion size; *p* < 0.05 (at FDR < 0.25) was considered significant. From these correlations, we also derived the so called gene significance (GS) measures, indicating the relevance of a particular gene with regard to each phenotypic trait (e.g., lesion size). We further used module membership (MM) calculations to identify highly connected 'hub' genes within the modules of interest based on their intra-modular gene connectivity (centrality). Finally, modules were used as input to the context likelihood of relatedness (CLR) algorithm to infer the so called transcription factor regulatory gene networks (TF-RGNs) [21] and identify their key driver genes [22]. For details, see the [Supplemental Methods](#).

2.3. Enrichment for risk association to coronary artery disease (CAD)

To distinguish between potentially causal vs. reactive modules, we calculated their so called CAD risk enrichment, as previously described [23]. For this, we first collected eSNPs for the corresponding module genes in seven metabolic and vascular human tissues (AAW: atherosclerotic arterial wall, IMA: internal mammary artery, Liver, SF: subcutaneous fat, SM: skeletal muscle, VF: visceral fat and WB: whole blood) obtained from 114 well-characterized CAD patients undergoing coronary artery bypass grafting surgery, which were part of the Stockholm Atherosclerosis Gene Expression (STAGE) study [24]. We then extracted their CAD association *p*-values from the CARDIoGRAMplusC4D GWAS meta-analysis dataset in 63,746 CAD cases and 130,681 controls [11]. These eSNPs were used to calculate fold enrichment and statistical significance for association with CAD in comparison to >10,000 random groups of SNPs, corrected for chromosome, gene density and major allele frequency. For further details, see the [Supplemental Methods](#).

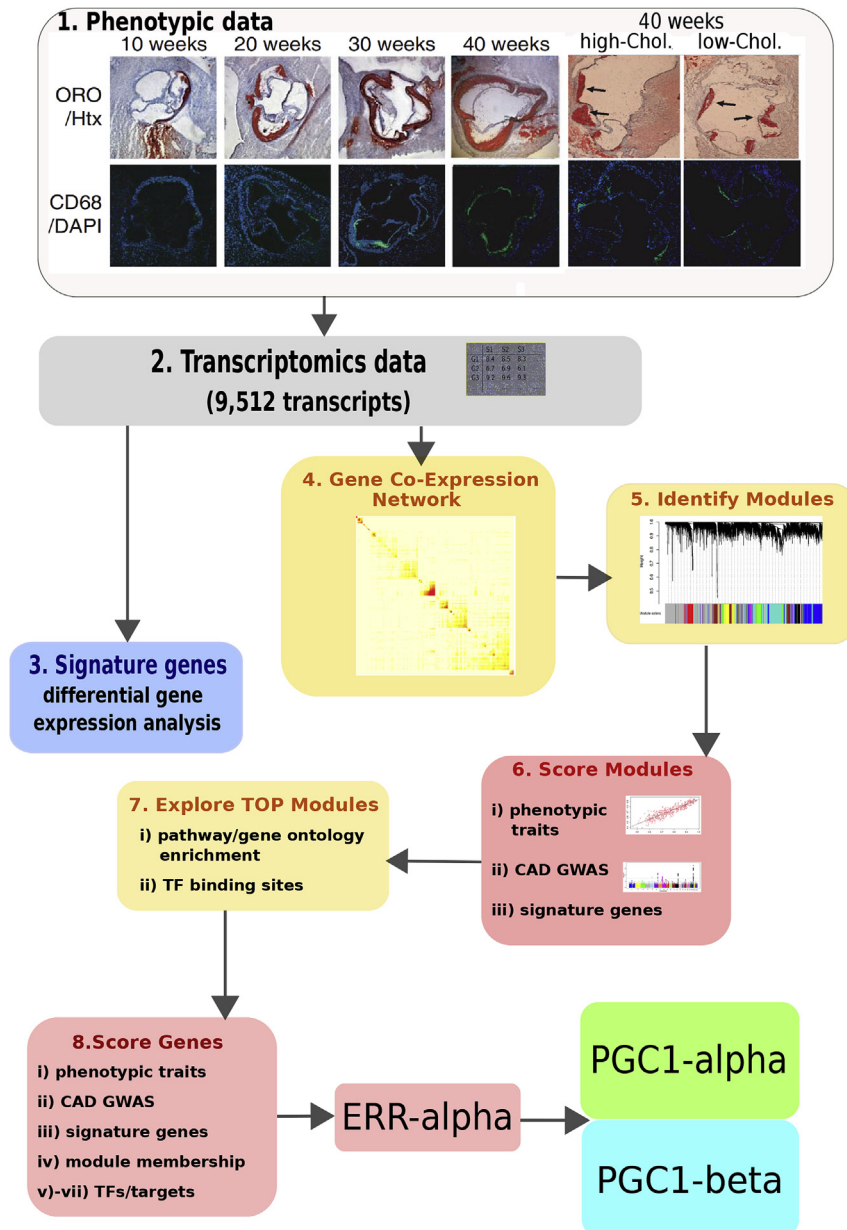


Fig. 1. Data used and workflow of the network approach identifying ERR- α /PGC-1 as key mitochondrial regulators in atherosclerotic lesion development.

1. Atherosclerosis progression in *Ldlr*^{-/-}*ApoB*^{100/100}*Mtpp*^{flax/flax} Mx1-Cre (Reversa) mice (left panel) and effect of plasma-cholesterol lowering at 30 weeks on lesion progression: representative sections of the aortic arch, stained with Oil-red-O (upper panels) or CD68 (lower panels) (from Ref. [9]). 2. Transcriptome data ($n = 9512$) pre-processing and filtering. 3. Identification of mitochondrial signature genes. 4. Gene co-expression network re-construction and 5. identification of modules. 6. Module ranking and 7. Exploring the top scoring modules. 8. Gene ranking from the top scoring modules to identify key mitochondrial regulators.

2.4. Functional enrichment analysis

Functional enrichment analysis was performed using ToppFun from the ToppGene suite [25], which detects functional enrichment in 14 annotation categories, including Gene Ontology (GO) terms, pathways, transcription factor-binding sites (TFBS), as well as small molecule- gene associations. In addition, we also examined ConsensusPathDB [26] pathways and CORUM [27] protein complexes.

2.5. Transcription factor binding site enrichment analysis

The analysis of putative transcription factor binding sites in promoter regions of genes was conducted using three different tools with default parameters: ToppFun [25], TransFind [28] and oPOSSUM [29].

3. Results

3.1. Identification of mitochondrial signature genes

The main focus of our analysis were the 1240 nuclear-encoded mitochondrial genes expressed during atherosclerosis progression, hereinafter referred to as mitochondrial genes. However, as mitochondria are involved in close communication with most other cellular components [4], we started our analysis using a global set of 9512 expressed genes, to subsequently investigate their representations of mitochondrial genes (2. in Fig. 1). First, we explored, whether there were statistically significant ($-1.0 \leq \log_2FC \leq 1.0$, at FDR < 0.25) changes in mitochondrial gene expression between the consecutive time points (i.e. 10 vs. 20, 20 vs. 30, 30 vs. 40 weeks of

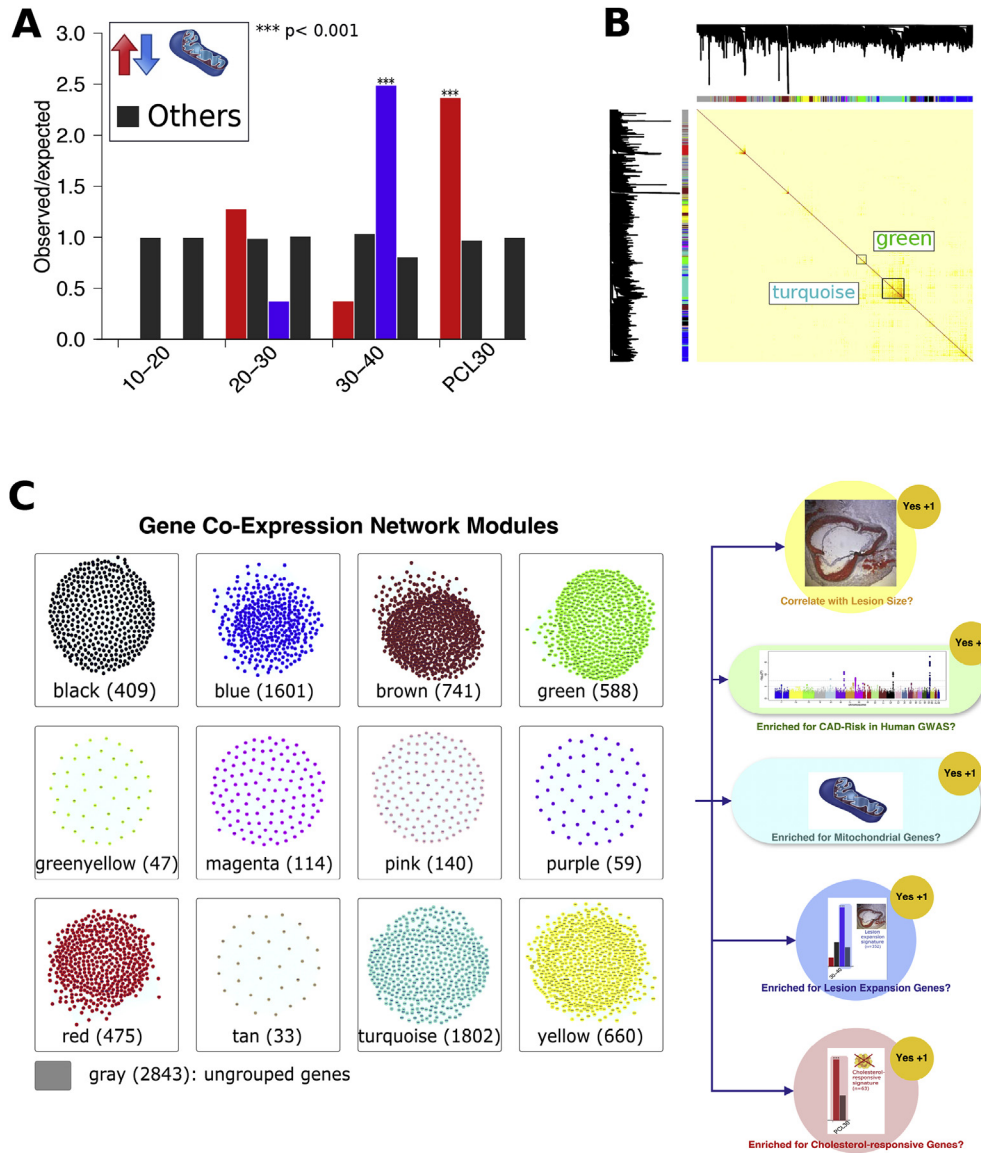


Fig. 2. Mitochondrial signature gene identification and co-expression network re-construction.

(A) Barplot showing the proportion of the observed vs. expected mitochondrial vs. non-mitochondrial genes (Others) among the up- and down-regulated genes during atherosclerosis progression or after genetically lowering plasma cholesterol at 30 weeks. PCL: plasma cholesterol lowering. (B) The topological overlap matrix (TOM) plot showing the WGCNA [20] co-expression network constructed using the 9512 expressed genes. Genes (rows and columns) are colored by their assignment to the 12 modules, corresponding to squares along the diagonal. (C) Scheme depicting module prioritization strategy: each module is assigned a score of +1 if it shows correlation to changes in atherosclerotic lesion size over time, enrichment in CAD risk and/or enrichment in mitochondrial genes.

age) and if so, what proportion of mitochondrial genes were involved, i.e. identify mitochondrial signature genes (3. in Fig. 1). We found that mitochondrial genes were significantly over-represented among the genes down-regulated between 30 and 40 weeks of age, involving 352 or >28% of all mitochondrial genes (2.5-fold, OR = 4.08, $p = 6.1 \times 10^{-72}$; '30-40' in Fig. 2A and Supplemental Fig. 6), including two members of the peroxisome proliferator-activated receptor γ co-activator 1 family of transcription regulators - PGC1- α and - β , well-known players in mitochondrial transcription programs [30]. Phenotypically, this coincided with the most rapid lesion expansion phase and foam cell formation: at 30 weeks mice displayed small lesions, which expanded markedly over the next 10 weeks, forming plaques that cover ~7.2% of the aortic tree ($p < 1.0 \times 10^{-4}$). In parallel, increasing numbers of monocytes/macrophages and foam cells were observed (1. left panel in Fig. 1, Supplemental Figs. 1 and 2, and ref. [9]).

Hence, we further refer to these genes as the *mitochondrial lesion expansion signature genes* (Supplemental Table 4). Interestingly, when lowering plasma cholesterol (PCL) at 30 weeks by >80% (from 427 to 54 ± 31 mg/L) using recombination of hepatic Mttp, 10 weeks later (i.e. at week 40) atherosclerotic lesion size was significantly decreased, as compared to the control animals exposed to high cholesterol (1. right panel in Fig. 1, Supplemental Fig. 3A, and refs. [9,10]). On the transcriptome level, a total of 204 genes were up-regulated after PCL [10], 30% ($n = 63$) of those were mitochondrial genes (2.4-fold enrichment, OR = 3.08, $p = 2.4 \times 10^{-11}$; 'PCL30' in Fig. 2A and Supplemental Fig. 6). We further refer to these genes as the *mitochondrial cholesterol-responsive signature genes* (Supplemental Table 5). In fact, the vast majority (73%) of mitochondrial genes up-regulated after cholesterol lowering belonged to those that were previously down-regulated during hypercholesterolemia and lesion expansion (46 genes; OR = 107.6,

$p < 6.4 \times 10^{-56}$), implying that mitochondria partly respond to changes in plasma cholesterol levels through the transcriptional suppression or activation, respectively. This is in line with the notion that mitochondria serve as sophisticated and dynamic responsive sensors of their local environment [31] and that this response is mainly achieved at the level of transcription [7]. On the other hand, however, 87% of the genes down-regulated during lesion expansion could not be re-induced by normocholesterolemia, suggesting that there may be mitochondrial processes that cannot be restored by lowering plasma cholesterol alone.

3.2. Gene co-expression network module identification and prioritization by scoring

To further explore the network context of mitochondrial signature genes, we performed the weighted gene co-expression network analysis (WGCNA, [20]; 4. and 5. in Figs. 1 and 2B) using the 9512 expressed genes. This yielded 12 genes modules, each of which given an arbitrary color name (the number of genes in parentheses): black (409), blue (1,601), brown (741), green (588), green yellow (47), magenta (114), pink (140), purple (59), red (475), tan (33), turquoise (1,802) and yellow (660). The gray module unified 2843 genes that could not be grouped in any particular community (Supplemental Table 7). Interestingly, PGC1- α was part of the green module, whereas PGC1- β was in the turquoise module.

Hence, we will further refer to the respective modules as the PGC1- α and PGC1- β modules. In order to prioritize modules by their relevance to atherosclerotic lesion progression and mitochondrial gene representations, we scored them (+1 or 0) in five different categories (6. in Figs. 1 and 2C):

- 1 We first correlated (Pearson's test) each module with changes in atherosclerotic lesion size over time in mice (1. left panel in Fig. 1, Supplemental Figs. 1 and 2, Supplemental Table 7, and Ref. [9]) and identified two modules - PGC1- α and PGC1- β - demonstrating significant negative correlation ($r = -0.42$ and -0.43 , respectively, at FDR < 0.25 ; Fig. 3A, Supplemental Tables 8 and 11, and Supplemental Fig. 8), indicating their atheroprotective role.
- 2 To distinguish between causal vs. reactive modules, we performed the so called disease risk enrichment analysis [23] (Fig. 3B and Supplemental Table 9) using human GWAS data of CAD [11], and expression-related SNPs in seven STAGE cohort [24] tissues (see Materials and methods). We scored a module +1 if it: (i) demonstrated a significant CAD risk enrichment across \geq three tissues (i.e. the genetic effects were "persistent" [23]) and (ii) one of these tissues was arterial wall or whole blood. The PGC1- β module was significantly enriched for CAD risk in blood (1.4-fold, $p = 8.1 \times 10^{-9}$), whereas the PGC1- α module

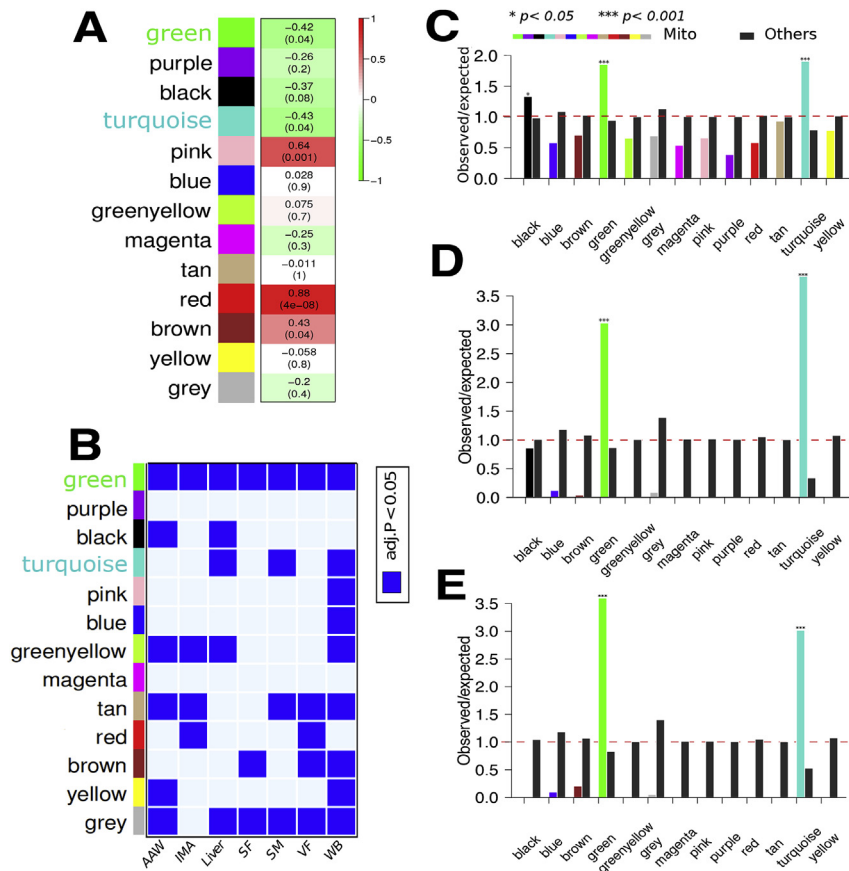


Fig. 3. Ranking modules by scoring and mitochondria-related module identification. (A) Module correlation to changes in atherosclerotic lesion size over time in mice [9]. (B) CAD-risk enrichment analysis results for the 12 modules (y-axis) using eSNPs overlapping with CAD-associated SNPs from GWAS [11] in seven metabolic and vascular human tissues (x-axis) from the STAGE study [24]: AAW: atherosclerotic arterial wall, IMA: internal mammary artery, Liver, SF: subcutaneous fat, SM: skeletal muscle, VF: visceral fat and WB: whole blood. Significant enrichments ($p < 0.05$) are shown in blue. (C) Module overlaps with mitochondrial ($n = 1240$), (D) mitochondrial lesion expansion ($n = 352$), and (E) cholesterol-responsive signature ($n = 63$) genes. In each case, the y-axis displays the observed vs. expected number of mitochondrial or mitochondrial signature genes, respectively. The colored bars of the x-axis represent the enrichment ratio for the 12 modules. For comparison, the black bars consider the non-module genes. Asterisks denote significant overlaps: * $p < 0.05$, *** $p < 0.001$. (For interpretation of the references to colour in this figure legend, the reader is referred to the web version of this article.)

displayed disease risk enrichment across all seven tissues (Fig. 3B).

- 3–5 To identify mitochondria-related modules, we calculated the overlaps of the 12 WGCNA module genes (Supplemental Table 6) with the expressed mitochondrial genes ($n = 1240$), mitochondrial lesion expansion ($n = 352$) and cholesterol-responsive ($n = 63$) signature genes (Supplemental Tables 2, 4 and 5, respectively). Both PGC1- α and PGC1- β modules were significantly enriched with all three mitochondrial gene sets (Fig. 3C–E and Supplemental Table 10) and scored +1 in the respective categories (Supplemental Table 11).

3.3. Exploring the top scoring PGC1- α and PGC1- β modules

In total, the PGC1- α and - β modules reached the highest possible score of five (Fig. 4A and Supplemental Table 11). Both modules negatively correlated with changes in atherosclerotic lesion size over time, displayed significant enrichment for CAD/atherosclerosis risk across multiple tissues, and were significantly enriched with mitochondrial genes, in particular, mitochondrial lesion expansion and cholesterol-responsive signature genes. In fact, the PGC1- α and - β modules were highly related to each other and part of the same meta-module (Fig. 4B). Taken together, these observations suggest that the two mitochondria-related modules might be important to protect against atherosclerosis, hence our further analysis focused on understanding their genes and pathways (7. in Fig. 1). In both modules, functional enrichment analysis (Fig. 4C and Supplemental Table 12) suggested that mitochondrial biogenesis might be affected, as we observed significant (at $FDR < 0.05$) overrepresentation of genes related to mitochondrion organization (involving synthesis of new mitochondrial components www.ebi.ac.uk/QuickGO/; 20% mitochondrial genes). We also observed enrichment of several key mitochondrial pathways, including mitochondrial fatty acid β -oxidation, TCA cycle, oxidative phosphorylation and electron transport chain (5–10% of mitochondrial genes), as well as the 55S, 39S and 28S mitochondrial ribosomal subunits, pointing to a possible decrease in mitochondria numbers, as ribosomal protein genes are commonly used as reference genes [32]. Finally, we observed enrichment of genes involved in homeostasis pathways of four common ROS (hydroxyl radicals, hydrogen peroxide, superoxide and peroxynitrite), comprising 10–30% of module mitochondrial genes. Considering that mitochondrial biogenesis is finely tuned at the level of transcriptional regulation [7], we analyzed putative transcription factor (TF) binding sites in promoter regions of mitochondrial genes (Fig. 4D and Supplemental Table 17) in the two modules (see Materials and methods for details) and found that these were enriched for the transcription factor estrogen related receptor ERR- α (*ESRRA*) binding sites (PGC1- α : 18 genes, $p = 1.1 \times 10^{-4}$ and PGC1- β : 47 genes, $p = 2.6 \times 10^{-7}$). Notably, the transcriptional activity of ERR- α is regulated by PGC1 co-activators, which convert it from a latent to a potent transcriptional activator [7]. Together, ERR- α /PGC1 are known to regulate a broad set of mitochondrial genes, including lipid oxidation genes, components of OXPHOS, TCA cycle, mitochondrial import and dynamics [7]. Most importantly, they are known as master regulators of mitochondrial biogenesis and antioxidant defenses [33,34], which is in line with our functional enrichment analysis results. In fact, ERR- α itself was part of the PGC1- α module (Supplemental Table 6).

3.4. Ranking PGC1- α and PGC1- β module genes to identify mitochondrial key regulators

In the third part of our analysis, we utilized the information

obtained from the first two parts and performed candidate gene selection by scoring (+1 or 0; 8. in Fig. 1):

- 1 First, we scored +1 all mitochondria-related genes from each module, assigning an additional score to lesion expansion genes (Fig. 3D) and cholesterol-responsive genes (Fig. 3E), respectively.
- 2 We additionally utilized two gene-level metrics [20] to prioritize genes: (i) gene significance (GS) to variation in atherosclerotic lesion size (i.e. correlation) and (ii) the so called module membership (MM) of a gene, which indicates, how strongly its expression correlates (i.e. is connected) with all other genes within that module to identify highly connected 'hub' genes. After selecting all significant measurements ($p < 0.05$, at $FDR < 0.25$, Supplemental Fig. 14 and Supplemental Table 14) in these categories, we divided them into quintiles and scored +1 those genes, which were within the upper-two (MM) or the lower-two quintiles (GS, mainly negative), respectively.
- 3 We scored +1 genes that had ROS-related GO annotations (246 genes; Supplemental Table 15).
- 4 We prioritized transcription regulators (i) from AnimalTFDB [35] (Supplemental Table 16), (ii) using the results from TF binding site analysis (Fig. 4D and Supplemental Table 17) and (iii) expression correlations ($r \geq 0.7$) of putative target genes to the respective TFs within each module.

The top scoring genes in the PGC1- α and PGC1- β modules are shown in Fig. 4E (for complete gene scoring results see Supplemental Figs. 11 and 12, Supplemental Table 13). In both modules, there were no genes that would score positively in all nine categories. Nine genes from the PGC1- α module and 12 genes from the PGC1- β module obtained a total score ≥ 7 . In fact, the PGC1 factors themselves were among the highest scoring genes in the respective modules: *PPARGC1A* (PGC1- α) obtained a total score of +8, whereas *PPARGC1B* (PGC1- β) scored +7. Finally, using an independent approach, by reconstructing the so called transcription factor regulatory gene networks (TF-RGNs) [21] and identifying their key drivers [22], we also identified PGC1- α and PGC1- β as the most significant mitochondrial key drivers (i.e., master regulators) of the respective modules (Supplemental Fig. 15 and Supplemental Table 18, see Materials and methods and Supplementary data for details), demonstrating the utility of our scoring approach.

4. Discussion

Mitochondrial damage leading to increased production of ROS may be a relevant intermediate mechanism by which hypercholesterolemia exacerbates atherosclerotic lesion formation [1,2]. Here, we used a systems-level network approach to investigate this in a time-resolved fashion *in vivo* during atherosclerotic lesion formation (between 10 and 40 weeks of age) by re-evaluating the transcriptome profiles previously collected in *Ldlr*^{-/-}*Apob*^{100/100}*Mttp*^{fllox/fllox} *Mx1*-Cre (Reversa) mice during hypercholesterolemia and after genetic lowering of plasma cholesterol [9,10]. We identified two, partly overlapping, mitochondrial signatures: one down-regulated during the most rapid atherosclerotic lesion expansion and foam cell formation, i.e. between 30 and 40 weeks of age, and the other one up-regulated after plasma cholesterol lowering at 30 weeks. Using a network approach to analyze transcriptome profiles in terms of their co-expressed gene modules, we identified two modules around these mitochondrial signature genes and their key regulators - ERR- α , PGC1- α and PGC1- β . Both modules also negatively correlated with changes in atherosclerotic lesion size over time and displayed significant enrichment for CAD/atherosclerosis

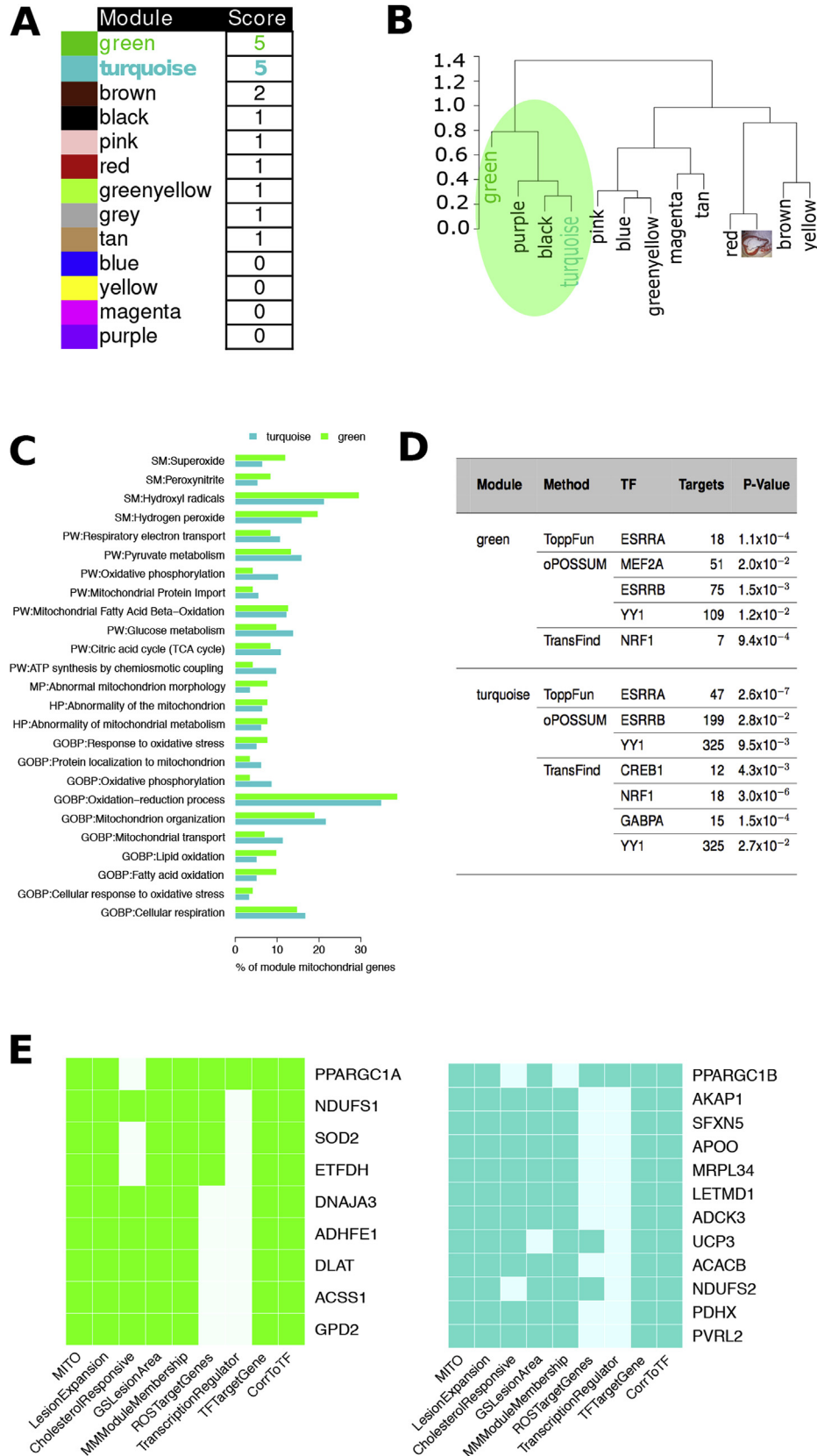


Fig. 4. Exploring the top scoring PGC1- α (green) and PGC1- β (turquoise) modules and ranking their genes to identify key mitochondrial regulators. (A) Module scoring results. (B) Hierarchical clustering dendrogram of module eigengenes demonstrating their relationships (i.e. correlations). (C) Functional enrichment analysis results of the module mitochondrial genes. PW: pathway, MP: mouse phenotype, HP: human phenotype, GOBP: Gene Ontology biological process, SM: small molecule, PPI: protein-protein interaction, CORUM: mammalian protein complex [27]. (D) Transcription factor binding sites enrichment analysis results for the module mitochondrial genes. (E) Top scoring genes (y-axis) in nine different categories (x-axis) for the PGC1- α and PGC1- β modules, respectively. Positive scores (+1) are shown in green and turquoise, respectively. (For interpretation of the references to colour in this figure legend, the reader is referred to the web version of this article.)

risk across multiple tissues, pointing to their possible atheroprotective role, which is in line with previous reports on PGC1- α - the best investigated member of the peroxisome proliferator-activated receptor γ co-activator 1 family of transcription regulators. Higher expression of PGC1- α has been reported to suppress VSMC migration [36], vascular inflammation [37], as well as macrophage-foam cell transition [38], mainly due to its involvement in cholesterol efflux pathways [39]. Moreover, the expression of PGC1- α was markedly decreased in human carotid atherosclerotic plaques compared to normal arteries [38,39] and inversely linked to disease progression [38]. In line with this, we also observed *PPARGC1A* among the down-regulated genes in the atherosclerotic as compared to the atherosclerosis-free arterial wall in the STAGE [24] cohort (Supplemental Fig. 13). So far, PGC1- β /ERR- α have only been implicated in macrophage polarization [40] and their role in atherogenesis remains to be investigated.

The above described functions of ERR- α /PGC1 factors can be partly attributed to their well-known roles as master regulators of mitochondrial biogenesis and antioxidant responses [30], decreasing the levels of ROS by supplying functioning mitochondria [37] and inducing antioxidant enzymes, such as superoxide dismutases (SODs) and the uncoupling proteins (UCPs) [37]. Indeed, in our data, the expression levels of *SOD2*, *UCP1* and *UCP3* tightly correlated with those of *ESRRA*, *PPARGC1A* and *PPARGC1B*. These findings are also in line with the functional enrichment analysis

results, where we observed over-representation of ROS homeostasis and key mitochondrial pathway (e.g., TCA cycle and OXPHOS) genes, indicating that mitochondrial biogenesis and antioxidative responses indeed might be diminished. Of note, however, PGC1 factors were not among the cholesterol-responsive genes, which is in part surprising as PGC1 expression was extensively increased in atrial muscle biopsies of patients on cholesterol-lowering statin therapy, however, this was accompanied by decreased ROS production [41], and recent studies actually suggest that statins may exert also antioxidative effects [41]. Similarly, in the aortic arch of *ApoE*^{-/-} mice, atorvastatin treatment significantly reduced ROS levels, while this was not true for lipid lowering by diet [42]. Hence, if the ROS levels remain high, lowering plasma cholesterol levels may not be sufficient to revert the suppression of PGC1 factors.

In Fig. 5 we summarize our findings in a hypothetical chain of events linking hypercholesterolemia to changes in mitochondrial transcriptome and subsequent atherosclerotic lesion formation. Based on previous studies, it is known that mitochondria are the main intracellular source of ROS [42] and that hypercholesterolemia progressively increases mitochondrial ROS production in the arterial wall [1,2]. What is also known, is that mitochondria themselves are targets of excessive ROS production and/or prolonged oxidative stress, leading to mitochondrial damage and loss-of-function. This happens, in part, by decreasing their antioxidative capacity and diminishing important quality control mechanisms,

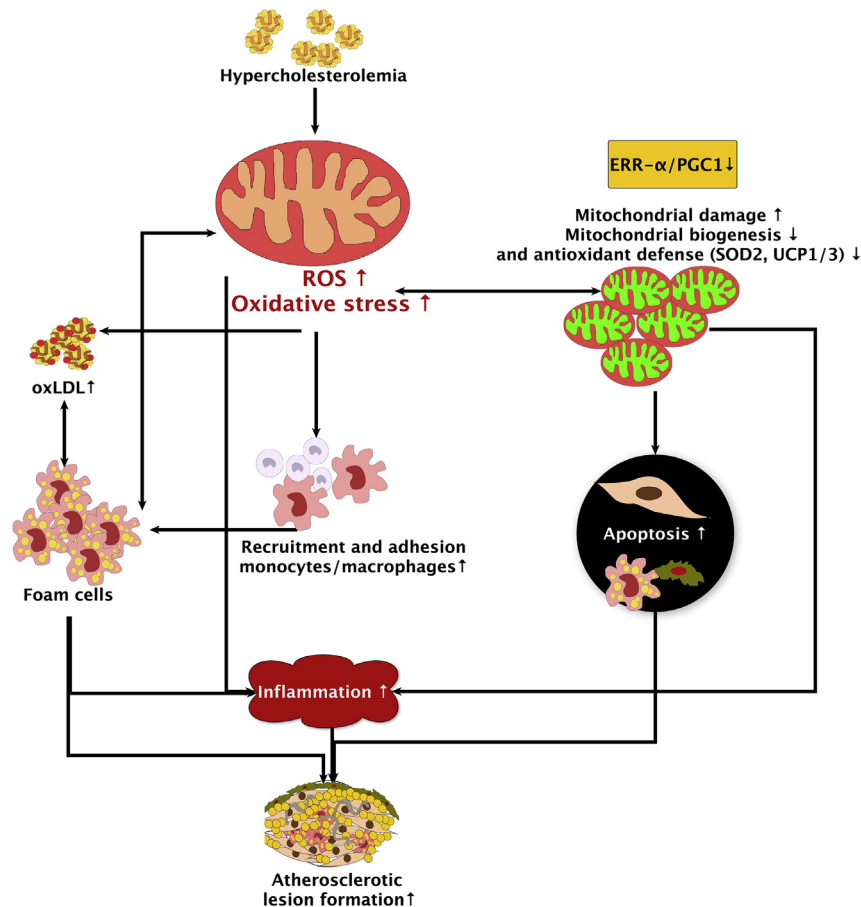


Fig. 5. Schematic presentation linking hypercholesterolemia to changes in mitochondrial transcriptome and subsequent atherosclerotic lesion formation.

Hypercholesterolemia progressively increases mitochondrial damage and ROS production in the arterial wall, which manifests itself as massive changes (decrease) in mitochondrial transcriptome including the down-regulation of key mitochondrial transcription regulators PGC1/ERR- α and their target genes (e.g., *SOD2* and *UCP3*). This leads to a decreased antioxidative capacity and diminishing of important quality control mechanisms, such as mitochondrial biogenesis. Accumulation of dysfunctional mitochondria may further increase ROS production, initiating a vicious cycle where ROS produced more ROS, triggering inflammatory responses and cell death in the arterial wall, and ultimately contributing to lesion development.

such as mitochondrial biogenesis, which is essential to replenish the damaged components [42]. Decrease in mitochondrial numbers and/or mitochondrial biogenesis would then manifest itself as massive changes (decrease) in mitochondrial transcriptome [7], observed in this study. Consequently, accumulation of dysfunctional mitochondria may further increase ROS production, initiating a vicious cycle where ROS produced more ROS, triggering inflammatory responses and cell death in the arterial wall, and ultimately contributing to lesion development [5].

In conclusion, our systems-level network analysis, linking time-resolved transcriptome data in atherosclerosis-prone hypercholesterolemic mice with CAD-associated eSNPs from human GWAS provides strong evidence that arterial wall responds to hypercholesterolemia by a coordinated down-regulation of mitochondrial genes. Moreover, these genes are tightly connected in co-expression network modules related to mitochondrial biogenesis and antioxidant responses, possibly regulated by *ERR- α /PGC1*, and supported as causal for CAD/atherosclerosis. Our study further supports the high predictive power of network strategies in identifying key regulatory genes and contributes to better understanding of the molecular processes leading to altered mitochondrial ROS metabolism in atherosclerosis, which could lead to more effective therapeutic strategies.

Conflict of interest

Johan L.M. Björkegren is the founder, main shareholder, and chairman of the board for Clinical Gene Networks (CGN).

Financial support

This study was supported by grants from the Fondation Leducq (CADgenomics: Under standing CAD Genes, 12CVD02), the German Federal Ministry of Education and Research (BMBF) within the framework of the e:Med research and funding concept (e:AtherosysMed, grant 01ZX1313A-2014), and the European Union Seventh Framework Programme FP7/2007–2013 under grant agreement n° HEALTH-F2-2013-601456 (CVgenes-at-target). Further grants were received from the DFG as part of the Sonderforschungsbereich CRC 1123 (B2).

Author contributions

HS and JB designed and supervised the research, and wrote the manuscript, BV designed the research, analyzed data, and wrote the manuscript; HF and HT analyzed data; JS and TK directed the design of analysis approaches. All authors participated in revising and editing the manuscript, and have read and approved the final version of the manuscript.

Appendix A. Supplementary data

Supplementary data related to this article can be found at <https://doi.org/10.1016/j.atherosclerosis.2017.10.019>.

References

- [1] S. Krause, et al., Increased generation of reactive oxygen species in mononuclear blood cells from hypercholesterolemic patients, *Thromb. Res.* 71 (1993) 237–240.
- [2] H.C.F. Oliveira, et al., Oxidative stress in atherosclerosis-prone mouse is due to low antioxidant capacity of mitochondria, *FASEB J.* 19 (2005) 278–280, <https://doi.org/10.1096/fj.04-2095fje>. <http://dx.doi.org/10.1096/fj.04-2095fje>.
- [3] N.R. Madamanchi, M.S. Runge, Mitochondrial dysfunction in atherosclerosis, *Circ. Res.* 100 (2007) 460–473, <https://doi.org/10.1161/01.RES.0000258450.44413.96>.
- [4] V.N. Kotiadis, M.R. Duchon, L.D. Osellame, Mitochondrial quality control and communications with the nucleus are important in maintaining mitochondrial function and cell health, *Biochim. Biophys. Acta* 1840 (2014) 1254–1265, <https://doi.org/10.1016/j.bbagen.2013.10.041>.
- [5] J. Gutierrez, S.W. Ballinger, V.M. Darley-Usmar, A. Landar, Free radicals, mitochondria, and oxidized lipids: the emerging role in signal transduction in vascular cells, *Circ. Res.* 99 (2006) 924–932, <https://doi.org/10.1161/01.RES.0000248212.86638.e9>.
- [6] Y. Wang, I. Tabas, Emerging roles of mitochondria ROS in atherosclerotic lesions: causation or association? *J. Atheroscler. Thromb.* 21 (2014) 381–390.
- [7] M.B. Hock, A. Kralli, Transcriptional control of mitochondrial biogenesis and function, *Annu. Rev. Physiol.* 71 (2009) 177–203.
- [8] M.M. Veniant, et al., Defining the atherogenicity of large and small lipoproteins containing apolipoprotein b100, *J. Clin. Invest.* 106 (2000) 1501–1510, <https://doi.org/10.1172/JCI10695>. <https://doi.org/10.1172/JCI10695>.
- [9] J. Skogsberg, et al., Transcriptional profiling uncovers a network of cholesterol-responsive atherosclerosis target genes, *PLoS Genet.* 4 (2008) e1000036, <https://doi.org/10.1371/journal.pgen.1000036>. <https://doi.org/10.1371/journal.pgen.1000036>.
- [10] J.L.M. Björkegren, et al., Plasma cholesterol-induced lesion networks activated before regression of early, mature, and advanced atherosclerosis, *PLoS Genet.* 10 (2014) e1004201, <https://doi.org/10.1371/journal.pgen.1004201>.
- [11] CARDIoGRAMplusC4D Consortium, P. Deloukas, et al., Large-scale association analysis identifies new risk loci for coronary artery disease, *Nat. Genet.* 45 (2013) 25–33, <https://doi.org/10.1038/ng.2480>.
- [12] R.C. Gentleman, et al., Bioconductor: open software development for computational biology and bioinformatics, *Genome Biol.* 5 (2004) R80, <https://doi.org/10.1186/gb-2004-5-10-r80>.
- [13] L. Gautier, L. Cope, B.M. Bolstad, R.A. Irizarry, affy—analysis of affymetrix genechip data at the probe level, *Bioinformatics* 20 (2004) 307–315, <https://doi.org/10.1093/bioinformatics/btg405>.
- [14] Z. Wu, R.A. Irizarry, R. Gentleman, F. Martinez-Murillo, F. Spencer, A Model Based Background Adjustment for Oligonucleotide Expression Arrays, Johns Hopkins University, Dept. of Biostatistics Working Papers, 2004.
- [15] A. Kauffmann, R. Gentleman, W. Huber, arrayqualitymetrics—a bioconductor package for quality assessment of microarray data, *Bioinformatics* 25 (2009) 415–416, <https://doi.org/10.1093/bioinformatics/btn647>.
- [16] G.K. Smyth, Linear models and empirical bayes methods for assessing differential expression in microarray experiments, *Stat. Appl. Genet. Mol. Biol.* 3 (2004), <https://doi.org/10.2202/1544-6115.1027>. Article3.
- [17] Y. Benjamini, Y. Hochberg, Controlling the false discovery rate: a practical and powerful approach to multiple testing, *J. R. Stat. Soc. Ser. B Methodol.* 57 (1) (1995) 289–300.
- [18] M. Ashburner, et al., Gene ontology: tool for the unification of biology: the gene ontology consortium, *Nat. Genet.* 25 (2000) 25–29, <https://doi.org/10.1038/75556>.
- [19] R.A. Fisher, On the interpretation of χ^2 from contingency tables, and the calculation of p, *J. R. Stat. Soc.* 85 (1) (1922) 87–94.
- [20] P. Langfelder, S. Horvath, Wgcna: an R package for weighted correlation network analysis, *BMC Bioinform.* 9 (2008) 559, <https://doi.org/10.1186/1471-2105-9-559>.
- [21] A. Madar, A. Greenfield, E. Vanden-Eijnden, R. Bonneau, Dream3: network inference using dynamic context likelihood of relatedness and the inferelator, *PLoS One* 5 (2010) e9803.
- [22] Z.J. Zhang Bin, Identification of Key Causal Regulators in Gene Networks, EMBO Press, 2013.
- [23] H. Foroughi Asl, et al., Expression quantitative trait loci acting across multiple tissues are enriched in inherited risk for coronary artery disease, *Circ. Cardiovasc. Genet.* 8 (2015) 305–315.
- [24] S. Hägg, et al., Multi-organ expression profiling uncovers a gene module in coronary artery disease involving transendothelial migration of leukocytes and lim domain binding 2: the stockholm atherosclerosis gene expression (stage) study, *PLoS Genet.* 5 (2009) e1000754, <https://doi.org/10.1371/journal.pgen.1000754>.
- [25] J. Chen, E.E. Bardes, B.J. Aronow, A.G. Jegga, Toppgene suite for gene list enrichment analysis and candidate gene prioritization, *Nucleic Acids Res.* 37 (2009) W305–W311, <https://doi.org/10.1093/nar/gkp427>.
- [26] A. Kamburov, U. Stelzl, H. Lehrach, R. Herwig, The consensuspathdb interaction database: 2013 update, *Nucleic Acids Res.* 41 (2013) D793–D800, <https://doi.org/10.1093/nar/gks1055>.
- [27] A. Ruepp, et al., Corum: the comprehensive resource of mammalian protein complexes—2009, *Nucleic Acids Res.* 38 (2010) D497–D501, <https://doi.org/10.1093/nar/gkp914>.
- [28] S.M. Kielbasa, H. Klein, H.G. Roider, M. Vingron, N. Blättgen, Transfind—predicting transcriptional regulators for gene sets, *Nucleic acids Res.* 38 (2010) W275–W280.
- [29] A.T. Kwon, D.J. Arenillas, R. Worsley Hunt, W.W. Wasserman, opossum-3: advanced analysis of regulatory motif over-representation across genes or chip-seq datasets, *G3 (Bethesda Md.)* 2 (2012) 987–1002.
- [30] Z. Wu, et al., Mechanisms controlling mitochondrial biogenesis and respiration through the thermogenic coactivator pgc-1, *Cell* 98 (1999) 115–124, [https://doi.org/10.1016/S0092-8674\(00\)80611-X](https://doi.org/10.1016/S0092-8674(00)80611-X).
- [31] X. Tang, Y.-X. Luo, H.-Z. Chen, D.-P. Liu, Mitochondria, endothelial cell function, and vascular diseases, *Front. Physiol.* 5 (2014) 175, <https://doi.org/10.3389/fphys.2014.00175>.
- [32] H.J.M. de Jonge, et al., Evidence based selection of housekeeping genes, *PLoS One* 2 (2007) e898, <https://doi.org/10.1371/journal.pone.0000898>.

- [33] Y. Kamei, et al., Ppargamma coactivator 1beta/err ligand 1 is an err protein ligand, whose expression induces a high-energy expenditure and antagonizes obesity, *Proc. Natl. Acad. Sci. U. S. A.* 100 (2003) 12378–12383, <https://doi.org/10.1073/pnas.2135217100>.
- [34] S.N. Schreiber, D. Knutti, K. Brogli, T. Uhlmann, A. Kralli, The transcriptional coactivator pgc-1 regulates the expression and activity of the orphan nuclear receptor estrogen-related receptor alpha (erralpha), *J. Biol. Chem.* 278 (2003) 9013–9018, <https://doi.org/10.1074/jbc.M212923200>.
- [35] H.-M. Zhang, et al., Animaltdb: a comprehensive animal transcription factor database, *Nucleic Acids Res.* 40 (2012) D144–D149, <https://doi.org/10.1093/nar/gkr965>.
- [36] A. Qu, et al., Pgc-1alpha attenuates neointimal formation via inhibition of vascular smooth muscle cell migration in the injured rat carotid artery, *Am. J. Physiol. Cell Physiol.* 297 (2009) C645–C653, <https://doi.org/10.1152/ajpcell.00469.2008>.
- [37] I. Valle, A. Alvarez-Barrientos, E. Arza, S. Lamas, M. Monsalve, Pgc-1alpha regulates the mitochondrial antioxidant defense system in vascular endothelial cells, *Cardiovasc. Res.* 66 (2005) 562–573, <https://doi.org/10.1016/j.cardiores.2005.01.026>.
- [38] C. McCarthy, et al., Macrophage ppar gamma co-activator-1 alpha participates in repressing foam cell formation and atherosclerosis in response to conjugated linoleic acid, *EMBO Mol. Med.* 5 (2013) 1443–1457, <https://doi.org/10.1002/emmm.201302587>.
- [39] D. Karunakaran, et al., Macrophage mitochondrial energy status regulates cholesterol efflux and is enhanced by anti-mir33 in atherosclerosis, *Circulation Res.* 117 (2015) 266–278.
- [40] J. Sonoda, et al., Nuclear receptor err alpha and coactivator pgc-1 beta are effectors of ifn-gamma-induced host defense, *Genes Dev.* 21 (2007) 1909–1920.
- [41] J. Bouitbir, et al., Opposite effects of statins on mitochondria of cardiac and skeletal muscles: a 'mitohormesis' mechanism involving reactive oxygen species and pgc-1, *Eur. Heart J.* 33 (2012) 1397–1407.
- [42] M. Ekstrand, et al., Imaging of intracellular and extracellular ros levels in atherosclerotic mouse aortas ex vivo: effects of lipid lowering by diet or atorvastatin, *PLoS One* 10 (2015) e0130898, <https://doi.org/10.1371/journal.pone.0130898>.